

## Increasing The Tensile Strength of Adhesive T-Type Joints with Bio-Inspired 3D Printed Inserts

Mirari Ğunav Geçit<sup>1</sup> , Tolga Topkaya<sup>2</sup> 

<sup>1</sup> Batman University, Mechanical Engineering Department, Batman, Turkey. (mirarigeçit@gmail.com)

<sup>2</sup> Batman University, Mechanical Engineering Department, Batman, Turkey. (tolga.topkaya@batman.edu.tr)

### ARTICLE INFO

Received: Feb., 24. 2022

Revised: Jan, 10. 2023

Accepted: Jan, 10. 2023

#### Keywords:

Adhesive

T-joint

Additive Manufacturing

3D Printing

Tensile Test

Corresponding author: *Tolga Topkaya*

ISSN: 2536-5010 / e-ISSN: 2536-5134

DOI: <https://doi.org/10.36222/ejt.1078345>

### ABSTRACT

In the present study, insert materials manufactured with a 3D printer were used to increase the strength of T-type adhesive joints, which have an important area of use in aviation and aerospace applications. Experiments were carried out for 3 different overlap lengths and bending radius values. In addition to the unreinforced samples, 4 different insert material designs were used for each overlap length: solid-reinforced model, hollow reinforced model, vertically reinforced model, and horizontally reinforced model. PLA was used as insert material and AL 5754 and 3M DP460 as adherend and adhesive respectively. As a result of the experiments, it was determined that the use of reinforcement material increased the joint strength significantly. It has been determined that the maximum strength increase was observed on the horizontally reinforced insert used sample.

### 1. INTRODUCTION

Joining process needed for combining materials to construct the structures. Different joining techniques can be used depending on application area and material type. While joining with rivets or bolts is preferred for the creation of heavy structures [1], [2], also, welding or soldering can be used for suitable materials [3]. Adhesive joints are preferred especially for low-weight applications and flat surface needs [4]. Different geometric designs are applied to increase joint strength because adhesive materials are weak against peeling stress. [5]. Temiz investigated bending behavior of bi-adhesively joined double strap joints [6]. Bahrami et al investigated the effect of notched adherends on the tensile strength of single lap adhesive joints [7]. Khaliki et al investigated the effect of joint geometry on the failure modes and behavior of sandwich T-joints [8]. Solmaz and Topkaya compared adhesively, pinned, and hybrid joints tensile strength [9].

Surface modifications can be applied to increase the bond strength. Adhered surface can be abraded with mechanical abrasers [10] or laser etching technique can also be applied [11]. Cardoso et al. investigated the effect of surface pre-treatment on the strength of CFRP T-joints [12]. With the developing nano material technology, adhesive joint strength can be improved with nano particles [13]. Çetkin

investigated tensile strength behavior of graphene nano particle (GNP) and nano fiber reinforced adhesive joints [14]. Gholami et al. investigated fracture behavior of multi wallet carbon nano tube (MWCNTs) and graphene oxide nanoplatelets (GONPs) reinforced adhesive joints [15].

T and L type connections are preferred in applications where non-parallel adherends are joined. T-type and L-type connections are prone to complex stresses due to their geometry. Supports can be embedded in the adherends to minimize stresses [16]. The stress concentrations can be prevented, and joint strength increased in T-type and L-type connections with smoother transitions [17]. However, attention should be paid to the effect of filling materials on sample weight [18]. Barzegar et al. investigated bending behavior of T-type joints. They reported that increasing the fiber content on the adherends increased strength of samples [19].

In this study, tensile strength behavior of T-type joints investigated experimentally. For increasing the joint strength 3D printed inserts used in delta regions. 4 different insert designs and 3 different overlap lengths were used to investigate the effect of insert geometry. Aluminum alloy (AL-5754) and 3M DP460 two-part epoxy adhesive was used as adherend and adhesive materials respectively.

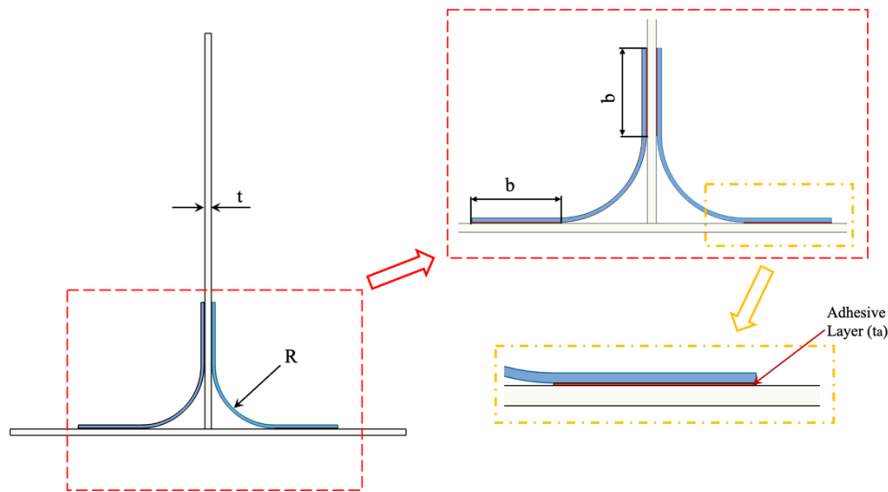


Figure 1. Dimensions of the test samples

## 2. MATERIALS AND METHODS

### 2.1. Materials and joint geometry

AL-5754 aluminum alloy was used as adherend material, and a two-part epoxy adhesive (DP460 from 3M) was used in the experiments. Mechanical properties of adherend and adhesive are given in table 1.

TABLE I  
MECHANICAL PROPERTIES OF MATERIALS [20], [21]

Property	AL-5754	3M DP460 Adhesive
Young's Modulus (GPa)	70300	2077.1
Poisson's Ratio	0.33	0.38
Tensile Strength (MPa)	245	44.616

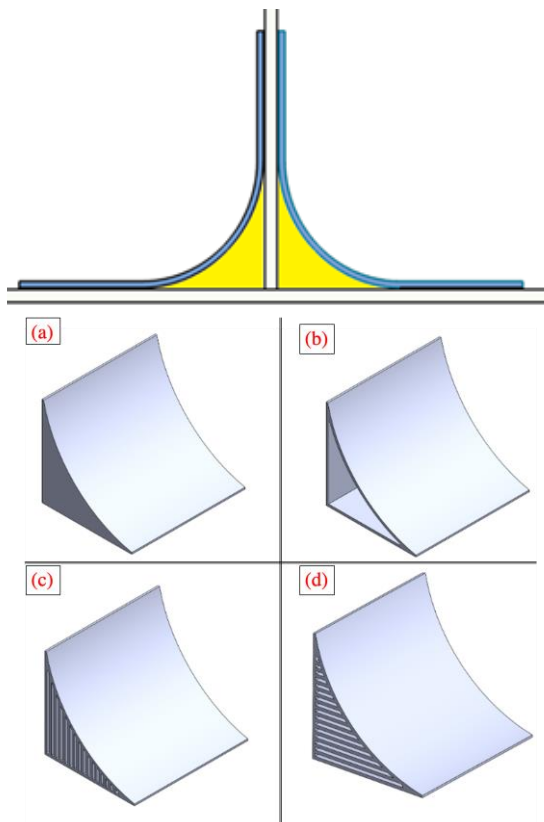


Figure 2. Delta regions and designed inserts a. solid reinforced model (SM) b. hollow reinforced model (HM) c. vertical reinforced model (VRM) d. horizontal reinforced model (HRM)

Four types of T-type joint have been used during the experiments. Dimensions of the T joints are given in Fig. 1. The dimensions of the vertical and horizontal adherends are identified as length ( $l=250$  mm), thickness ( $t=2$  mm) and width ( $w=25$  mm). Adhesive layer thickness ( $t_a$ ) was selected as 0.25 mm. The dimensions of the support materials are defined as overlap length ( $b= 10, 20$  and 30 mm), the bend radius ( $R= 5$  mm, 10 mm, and 15 mm).

### 2.2. Joint preparation and Experiments

Bonding surfaces were abraded with using 180 grid sandpapers. Then, the adherends and the supports were cleaned of oil and dirt with acetone. After the acetone used has evaporated from the surface, the bonding process with adhesive is completed. In order to provide the sample dimensions, a mold produced with a 3D printer was used during bonding applications. The delta regions between the bending regions of the support materials and the horizontal and vertical adherends were filled with inserts produced with a 3D printer using PLA filament. 5 different connection models were produced: non-reinforced model (NM), solid-reinforced model (SM), hollow reinforced model (HM), vertically reinforced model (VRM), horizontally reinforced model (HRM).

For filling the delta regions four different inserts were designed and printed with Crealty CR 10S Pro brand 3D printer. Printer settings were selected as 100 % for infill, 0.2 mm as layer height, and 50 mm/s as printing speed. Delta regions of T joint and designed insert materials are given in Fig. 2.

Samples were tested with Shimadzu universal testing equipment using 5 kN loadcell. The crosshead speed was selected as 1 mm/min. Test data was recorded at 10 Hz. For fixing the samples a homemade fixture was manufactured. The distance between lower support screws was selected as 125 mm. Every test repeated three times and average values used. Experimental setup is given in Fig. 3.



Figure 3. Experimental setup and application of the force

3. RESULTS AND DISCUSSION

Displacement as a function of applied force for different reinforcement material geometries of the samples with 10 mm overlap length and bending diameter samples is given in Fig. 4. Tensile failure load of the non-reinforced model (NM) was observed as 83.906 N. The failure load of the solid insert reinforced model (SM) is increased by 322% and it has 278.906 N value. Hollow insert reinforced models (HM) failure load is increased 645% according to the NM model and 542.031 N failure load is observed. The failure load of sample reinforced with vertically reinforced insert (VRM) is 588.594 N and the failure load of sample reinforced with horizontally reinforced insert (HRM) is 646.938 N. The damage load of VRM and HRM samples increased by 702% and 771%, respectively, compared to the NM sample. According to Burns et al., cracking starts at low load levels due to stress concentration in traditional samples, while bio-inspired T-joints have higher failure loads [22].

The applied force – displacement graph for different insert material geometries with a 20 mm overlap length and bending diameter is shown in Fig. 5. The NM has a tensile failure load of 77.031 N. Compared to the NM model, the failure load of the SM is increased by 440 %. HM, VRM, and HRM have tensile failure loads as 633.438 N, 772.66 N, and 858.906 N, respectively. Maximum failure load increase observed in HRM, the failure load increase is 1115% according to NM.

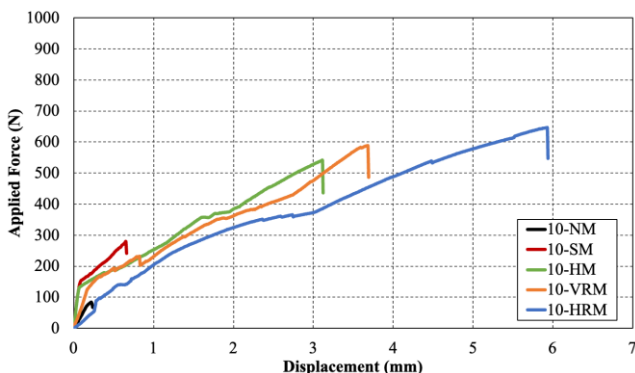


Figure 4. The effect of reinforcement material geometry on specimens' strength for 10 mm overlap length and radius diameter

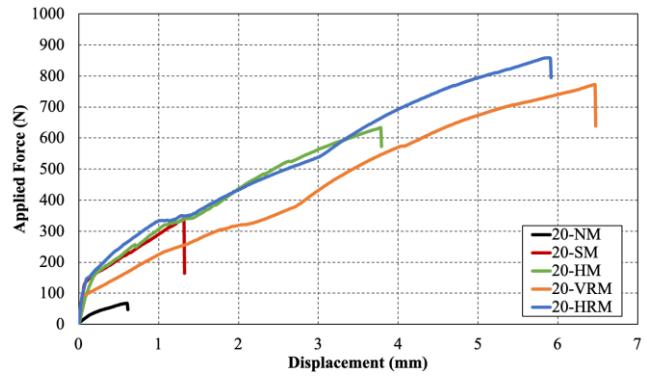


Figure 5. The effect of reinforcement material geometry on specimens' strength for 20 mm overlap length and radius diameter

Fig. 6 shows the applied force – displacement graph of 30 mm overlap length and bending diameter samples for different reinforcement geometries. Failure load of NM is observed as 63.125 N. failure loads for SM and HM are 498.438 N and 712.969 N respectively. The failure load of VRM is 910.938 N, and the failure load of HRM is 922.344 N. The damage load of VRM and HRM samples increased by 1443% and 1461%, respectively, compared to the NM sample.

Failure loads and sample weights are given in Fig. 7. Maximum sample weights are observed on SM while minimum sample weights are observed on non-reinforced samples. VRM and HRM models has same weights. Sample weights increased with increasing overlap length and bending diameter.

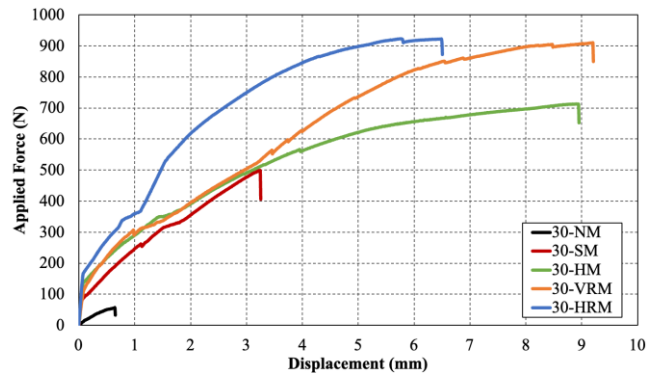


Figure 6. The effect of reinforcement material geometry on specimens' strength for 30 mm overlap length and radius diameter

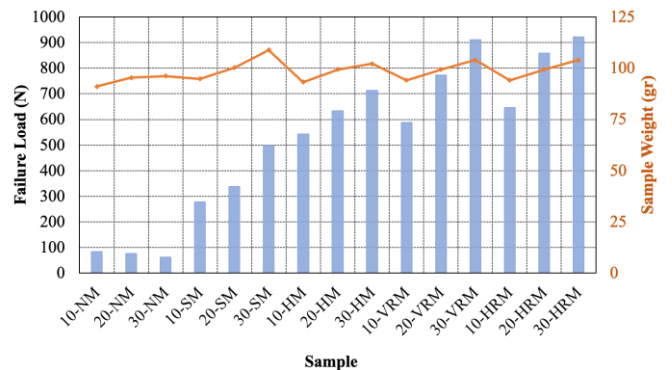


Figure 7. Variation of failure load with sample weight

Failure surfaces for non-reinforced model (NM) is given in Fig. 8. It has been determined that the main failure type is cohesion failure for all overlap lengths and bending diameters. Although adhesion failure was also observed in some parts of the joints, this type of failure was limited.



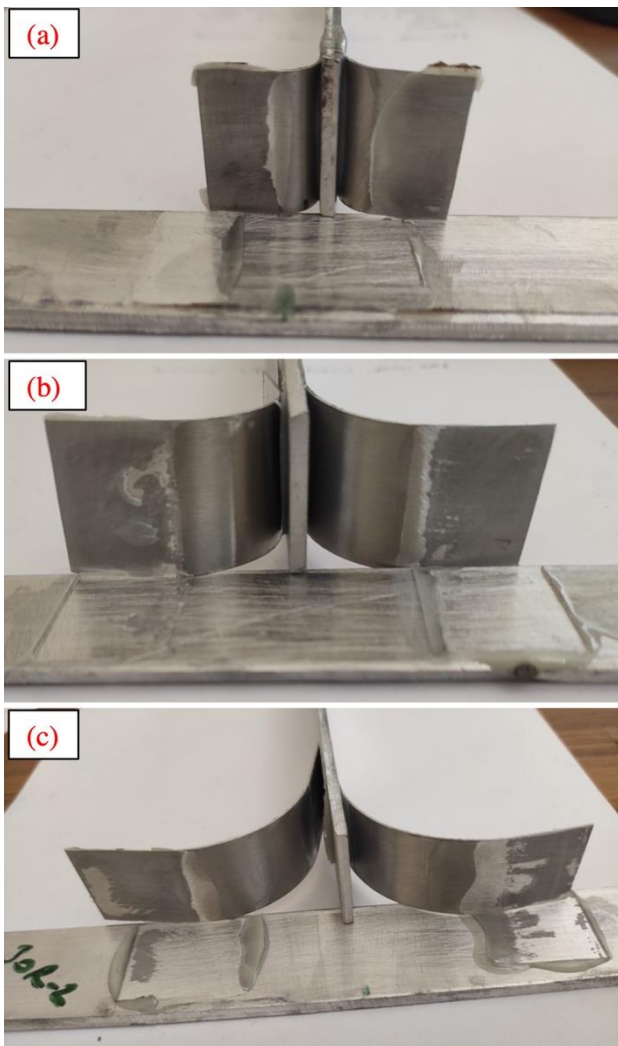


Figure 8. Failure surfaces of non-reinforced model (NM) a. 10 mm overlap length b. 20 mm overlap length c. 30 mm overlap length

Fig. 9 shows the failure surfaces of SM, HM, VRM and HRM with 20 mm overlap length. Cohesion failure is the main failure type for SM. It was determined that the adhesive material remained on the reinforcement material and separated from the aluminum adherend. This situation was evaluated to mean that the adhesive material adheres better to the reinforcing material. Cohesion failure was observed as main failure type for HM. There is minor damage on the insert material. The size of the damage seen in the insert material increased in HM samples with 20 mm overlap length and bend diameter. During the test, damage occurred on the left insert material, and then permanent joint failure occurred. In the specimen with 30 mm overlap length and bend diameter, both reinforcement materials on the right and left sides were damaged. If the thickness of the reinforcement material is higher than 0.25 mm, it is evaluated that the reinforcement material will not be damaged, and the joint strength will take higher values. Cohesion failure is observed as a main failure type for VRM samples. Adhesion failure type is also observed between reinforcement material and horizontal adherend interface for 30 mm overlap length and bending radius. It was observed that the main failure type was cohesion failure for 10 mm overlap length and bend diameter for HRM samples. In the sample with 20 mm overlap length and bend diameter, cohesion failure was observed in a limited area, while insert material damage was also observed. In the sample with 30 mm overlap length and bend diameter, it was determined that the adhesion failure covered a significant area, while the right insert material was damaged. Burns et al. reported that despite higher failure loads observed in bio-inspired samples, earlier onset of damage initiation [23].

No damage was observed in the 3D printed insert materials in any of the SM and VRM samples. The 3D printed inserts were damaged at all overlap lengths of the HM specimens. As the overlap length increased in the HRM specimens, the amount of damage seen in the 3D printed reinforcements increased.

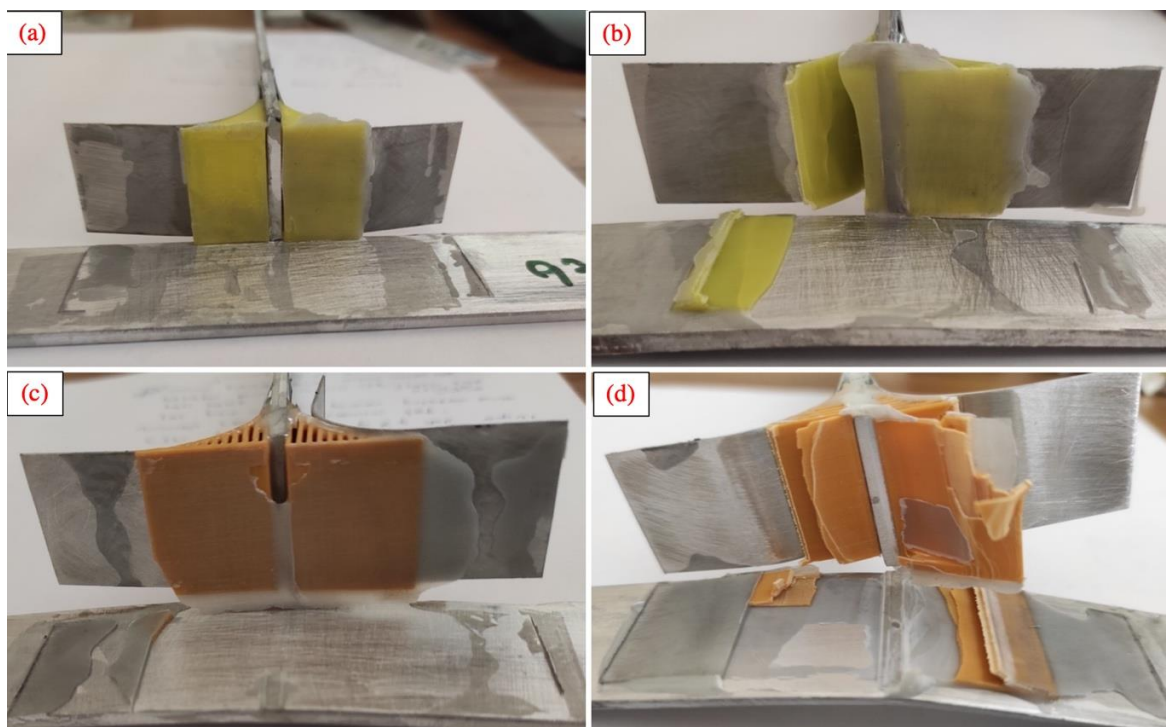


Figure 9. Failure surfaces for different insert designs a. solid-reinforced (SM), b. hollow reinforced (HM), c. vertically reinforced (VRM), d. horizontally reinforced (HRM).

#### 4. CONCLUSION

Tensile strength of adhesive T-type joints with 3D printed inserts at the delta region were investigated experimentally. Following conclusions can be made according to limited studies results.

- In the samples without insert material, the strength of the sample decreased with increasing the overlap length and bend diameter. The increase of the bend diameter caused this situation by increasing the moment value in the adhesive layer.

- The specimen strength increased with increasing overlap length and bend radius in the samples with 3D printed inserts.

- The maximum increase in strength was observed in the samples with solid inserts compared to the non-reinforced samples with an overlap length of 30 mm and a bend diameter. The amount of increase is 790%.

- In the samples with hollow insert material, the increase for 10 mm overlap length and bend diameter is 646%, the increase for 20 mm overlap length and bend diameter is 822%, and the increase for 30 mm overlap length and bend diameter is 1130%.

- The highest increase in strength was observed in the samples with vertically and horizontally reinforced inserts. The maximum failure load was observed in the sample with horizontally reinforced insert and 30 mm overlap length and bend diameter. This model provided a 1461% increase in strength compared to the non-reinforced model.

#### REFERENCES

- [1] U. A. Khashaba, T. A. Sebaey, and A. I. Selmy, "Experimental verification of a progressive damage model for composite pinned-joints with different clearances," *International Journal of Mechanical Sciences*, vol. 152, pp. 481–491, Mar. 2019, doi: 10.1016/j.ijmecsci.2019.01.023.
- [2] A. A. Abd-Elhady, S. Mousa, W. H. Alhazmi, H. E. M. Sallam, and M. Atta, "Effects of composite patching on cyclic crack tip deformation of cracked pinned metallic joints," *Journal of Adhesion*, vol. 97, no. 16, pp. 1561–1577, 2021, doi: 10.1080/00218464.2020.1803843.
- [3] E. Çetkin, Y. H. Çelik, and Ş. Temiz, "Effect of welding parameters on microstructure and mechanical properties of AA7075/AA5182 alloys joined by TIG and MIG welding methods," *Journal of the Brazilian Society of Mechanical Sciences and Engineering*, vol. 42, no. 1, Jan. 2020, doi: 10.1007/s40430-019-2119-7.
- [4] J. P. A. Valente, R. D. S. G. Campilho, E. A. S. Marques, J. J. M. Machado, and L. F. M. da Silva, "Geometrical optimization of adhesive joints under tensile impact loads using cohesive zone modelling," *International Journal of Adhesion and Adhesives*, vol. 97, Mar. 2020, doi: 10.1016/j.ijadhadh.2019.102492.
- [5] M. A. Morgado, R. J. C. Carbas, E. A. S. Marques, and L. F. M. da Silva, "Reinforcement of CFRP single lap joints using metal laminates," *Composite Structures*, vol. 230, no. September, p. 111492, 2019, doi: 10.1016/j.compstruct.2019.111492.
- [6] Ş. Temiz, "Application of bi-adhesive in double-strap joints subjected to bending moment," *Journal of Adhesion Science and Technology*, vol. 20, no. 14, pp. 1547–1560, 2006, doi: 10.1163/156856106778884262.
- [7] B. Bahrami, M. R. Ayatollahi, M. J. Beigrezaee, and L. F. M. da Silva, "Strength improvement in single lap adhesive joints by notching the adherends," *International Journal of Adhesion and Adhesives*, vol. 95, no. June, p. 102401, 2019, doi: 10.1016/j.ijadhadh.2019.102401.
- [8] S. M. R. Khalili, A. Ghaznavi, and A. Ghaznavi, "Effect of joint geometry on the behavior and failure modes of sandwich T-joints under transverse static and dynamic loads," *Journal of Adhesion*, vol. 91, no. 3, pp. 154–176, Mar. 2015, doi: 10.1080/00218464.2013.855881.
- [9] M. Y. Solmaz and T. Topkaya, "Progressive failure analysis in adhesively, riveted, and hybrid bonded double-lap joints," *Journal of Adhesion*, vol. 89, no. 11, 2013, doi: 10.1080/00218464.2013.765800.
- [10] A. Rudawska, "Selected aspects of the effect of mechanical treatment on surface roughness and adhesive joint strength of steel sheets,"

*International Journal of Adhesion and Adhesives*, vol. 50, pp. 235–243, Apr. 2014, doi: 10.1016/j.ijadhadh.2014.01.032.

- [11] E. G. Baburaj, D. Starikov, J. Evans, G. A. Shafeev, and A. Bensaoula, "Enhancement of adhesive joint strength by laser surface modification," *International Journal of Adhesion and Adhesives*, vol. 27, no. 4, pp. 268–276, Jun. 2007, doi: 10.1016/j.ijadhadh.2006.05.004.
- [12] J. v. Cardoso, P. v. Gamboa, and A. P. Silva, "Effect of surface pretreatment on the behaviour of adhesively-bonded CFRP T-joints," *Engineering Failure Analysis*, vol. 104, no. June, pp. 1188–1202, 2019, doi: 10.1016/j.engfailanal.2019.05.043.
- [13] İ. Saraç, H. Adin, and Ş. Temiz, "A research on the fatigue strength of the single-lap joint joints bonded with nanoparticle-reinforced adhesive," *Welding in the World*, vol. 65, pp. 635–642, 2021, doi: 10.1007/s40194-020-01063-2/Published.
- [14] E. Çetkin, "Determination of the effects of GNP and nano-fibers on bonding joints," *Journal of Manufacturing Processes*, vol. 71, pp. 27–36, Nov. 2021, doi: 10.1016/j.jmapro.2021.09.013.
- [15] R. Gholami, H. Khoramishad, and L. F. M. da Silva, "Glass fiber-reinforced polymer nanocomposite adhesive joints reinforced with aligned carbon nanofillers," *Composite Structures*, vol. 253, no. July, p. 112814, 2020, doi: 10.1016/j.compstruct.2020.112814.
- [16] S. Akpınar, M. D. Aydın, Ş. Temiz, and A. Özel, "3-D non-linear stress analysis on the adhesively bonded T-joints with embedded supports," *Composites Part B: Engineering*, vol. 53, pp. 314–323, Oct. 2013, doi: 10.1016/j.compositesb.2013.04.049.
- [17] R. Akrami, S. Fotouhi, M. Fotouhi, M. Bodaghi, J. Clamp, and A. Bolouri, "High-performance bio-inspired composite T-joints," *Composites Science and Technology*, vol. 184, no. September, p. 107840, 2019, doi: 10.1016/j.compscitech.2019.107840.
- [18] L. A. Burns, A. P. Mouritz, D. Pook, and S. Feih, "Strength improvement to composite T-joints under bending through bio-inspired design," *Composites Part A: Applied Science and Manufacturing*, vol. 43, no. 11, pp. 1971–1980, 2012, doi: 10.1016/j.compositesa.2012.06.017.
- [19] M. Barzegar, M. D. Moallem, and M. Mokhtari, "Progressive damage analysis of an adhesively bonded composite T-joint under bending, considering micro-scale effects of fiber volume fraction of adherends," *Composite Structures*, vol. 258, Feb. 2021, doi: 10.1016/j.compstruct.2020.113374.
- [20] M. Y. Solmaz and T. Topkaya, "The flexural fatigue behavior of honeycomb sandwich composites following low velocity impacts," *Applied Sciences (Switzerland)*, vol. 10, no. 20, 2020, doi: 10.3390/app10207262.
- [21] İ. Saraç, H. Adin, and Ş. Temiz, "Experimental determination of the static and fatigue strength of the adhesive joints bonded by epoxy adhesive including different particles," *Composites Part B: Engineering*, vol. 155, no. July, pp. 92–103, 2018, doi: 10.1016/j.compositesb.2018.08.006.
- [22] L.A. Burns, A.P. Mouritz, D. Pook, S. Feih, "Strength improvement to composite T-joints under bending through bio-inspired design" *Composites: Part A*, vol. 43 1971-1980, 2012, doi: 10.1016/j.compositesa.2012.06.017.
- [23] L. A. Burns, A.P. Mouritz, D. Pook, S. Feih, "Bio-inspired design of aerospace composite joints for improved damage tolerance" *Composite Structures*, vol. 94 995-1004, 2012, doi: 10.1016/j.compstruct.2011.11.005.

#### BIOGRAPHIES

**Mirari Ğunav Geçit** obtained her BSc degree in mechanical engineering from Harran University in 2018. She received the MSc. diploma in Mechanical Engineering from the Batman University in 2021. Her research interests are solid mechanics, adhesive materials, additive manufacturing and composite materials.

**Tolga Topkaya** graduated from Department of Mechanical Engineering at Fırat University in 2007. He gained his Ph.D. degree at the same university in 2017. He is working as Assistant Professor at Department of Mechanical Engineering, Batman University. He is a postdoctoral researcher in Aerospace Engineering Department at the University of Illinois at Urbana Champaign. His main research fields are composites, biomechanics and adhesion and adhesives.